

# Analysis of Wet Antenna Losses on 11.843 GHz Slant Path in Nigeria and Comparison with Some Tropical Climates

A. Y. Abdulrahman 

Department of Electrical & Electronics Engineering, University of Ilorin, P.M.B. 1515, Nigeria  
[abdulrahmanyusuf35@gmail.com](mailto:abdulrahmanyusuf35@gmail.com)

**Abstract**—The amount of water deposits on the receiving dish antenna can cause additional losses and consequently contaminate the actual slant-path attenuation. Only a few research works have been reported in the literature on the measurement of wet antenna attenuation (WAA) and the technique(s) of extracting the losses from the total attenuation in tropical and equatorial climates, characterized with heavy rainfall intensities of convective kind. Therefore, the adverse effects of antenna losses due to rain on a 11.843 GHz satellite link and the methodology of extracting the losses from the measured rain-induced attenuation have been reported in this article. A vertically polarized parabolic dish with diameter and elevation of 0.3 m and 42°, respectively have been used in the study. The measured results at 11.843 GHz were frequency-scaled in order to obtain their equivalents at 18.585 and 20.2 GHz; and then compared with those reported from Malaysia and Canada. The study will provide useful information in the planning and designing of an efficient and reliable Earth-satellite communication link in tropical climates. The experimental results also can further enrich the ITU-R databank.

**Index Terms**—direct-to-home broadcasting, drop size distribution, extraction techniques, frequency scaling, WAA.

## I. INTRODUCTION

Propels in satellite-based digital television systems have encouraged tremendous increase in the usage of the Ku- and Ka-bands for direct-to-home (DTH) broadcasting services. At such frequencies, various severe tropospheric effects, such as scintillation, rain-induced attenuation, cloud attenuation etc, adversely affect signal propagation by degrading both the signal strength and quality. However, attenuation due to rainfall is the most significant, as raindrops cause considerable attenuation of a radio signal at millimeter wavelengths which is directly responsible for link outages on Ku band signal [1], [2]. The slant-path attenuation does not only affect the end user's resulting performance, but also leads to a higher cost per bit of transmission [3]. Hence, the determination of attenuation due to rainfall plays a significant role in the design of earth-satellite link at frequencies above 10 GHz [4] - [6].

The slant-path attenuation is usually represented by the total measured data. However, the measured attenuation can be contaminated with some other losses as reported in [7]-[12]. As reported in [3], such losses are modeled as WAA; and are due to the combination of two effects, namely the: (i) antenna loss resulting from water film formed on the feed aperture surface and (ii) water pool accumulation on the main reflector. WAA is an additional contributor to the overall signal fading during rain event along the communication link. It is therefore undesirable as it adversely contributes to the overall signal fading during rain events. For this reason it must be subtracted from the measured total attenuation in order not to contaminate the actual propagation losses along the link.

Some experimental results on WAA statistics at Ku and Ka-bands can be found in the literature [3], [7]-[12]. Some early works on the study and modelling of WAA include the ACTS propagation experiments where water was sprayed on the ACTS propagation terminal (APT) antenna reflector. Another reported study was the experiment conducted on the feed window in the fall of 1993 after satellite transmissions were acquired. As reported in [12], the losses due to water droplets on the reflector were 1.0 and 1.9 dB at 20.2 and 27.5GHz, respectively, while those due to water droplets on the feed were generally less than 0.3 dB.

A water cell can cause signal degradation at four identified regions as defined Acosta *et. al* [13], where the ACTS satellite was used to measure the effects of a spherical water cell placed at each of these locations. The cell has diameter and volume of 0.35 m and 1.56 inches, respectively, while the parabolic reflector used in the experiment has an offset feed and  $F/D = 0.6$ . The measured WAA ranged from 0.25 dB to 9.5 dB across the 4 regions.

The results of the measurement of WAA on 26 GHz terrestrial microwave link at Universiti Teknologi Malaysia (UTM), Malaysia were presented in [7]. Wet radome experiments were performed on enclosing 2-foot parabolic dish, using water spray to simulate four types of testing, namely splashing, sheeting, rivulet and droplet tests. In this study, the WA scenario was emulated by using water spray for rain simulation. The WA losses obtained from the experiment were in the range 0.4 - 3 dB at 0.01% of time. It was assumed in the study that the water thickness was located randomly all over the radome; whereas in real-life situation, the water layer thickness is unknown and varies across the dish. Therefore, it is more practical to analytically relate the water thickness with the rain rate [13].

The analysis of correction of wet antenna attenuation (WAA) without dedicated rainfall monitoring for a set of 16 commercial microwave links (CMLs) was presented in [2]. The performance of six empirical WAA models was studied using data collected from over 53 rainfall events. As reported in the study, the model parameters for deriving WAA explicitly from rainfall intensity do not depend on the CML frequency and path length. Hence, the models are exportable to other locations with CMLs of similar antenna properties and probably almost similar propagation characteristics. Furthermore, it was suggested in [14]-[16] that the additional attenuation caused by WA for most rain intensities is relatively constant for a given CML. However, this claim cannot be established as studies have shown

that the WAA is largely dependent on the rainfall rate (and hence, the rain-induced path attenuation) [7], [11].

Rather than using a predefined constant value, J. Ostrometzky, et al [17] assumed that the WAA saturation value be treated as a random variable with a known expected value and variance, under highly controlled experimental conditions. More so, it was predicted in [18], that an increased number of E-band (60 – 90 GHz) CMLs are likely to be deployed in the nearest future. Consequently, the effects of WA should critically be taken into consideration in the future network designs especially in the estimation of fade margins, since E-band CMLs are more sensitive to weather-induced impairments compared to the Ku- and Ka-bands.

F. Martin, et al [19] estimated the WAA from the complimentary cumulative distribution function (CCDF) of measured attenuation and calculated raindrop path attenuation. The maximum value of WAA observed during extremely high intensity rainfalls ( $R \approx 70-130 \text{ mm/h}$ ) was in the range of 6 – 9 dB. Thus the claim in [14]-[16], that WAA assumed a constant value, was further discredited by the results reported in [19]. It should be noted that the constant WAA assumption might result in a significant overestimation of rainfalls retrieved from the CMLs. Other related works on WAA studies can be found in [20]-[22].

## II. THEORETICAL BACKGROUND

### A. Slant-path Attenuation

Slant-path attenuation  $A(\text{dB})$  is defined as the product of specific attenuation  $\lambda_R(\text{dB/km})$  and the effective slant-path, that is,  $A = \lambda_R L_E$ . The simplest method of evaluating  $\lambda_R(\text{dB/km})$  assumes that raindrops are spheres of homogeneous complex dielectric constant, randomly distributed in space with uniform density [23]. For engineering and other scientific applications, the relationship between  $\lambda_R$  and  $R(\text{mm/h})$  can be well approximated by the power law in the ITU-R 838-19 [23].

$$\lambda_R = k R^\alpha \quad (1)$$

Parameters  $k$  and  $\alpha$  are dependent on frequency, drop size distribution (DSD), temperature and polarization of the radio wave. Their values can be obtained from ITU-R 838-19; and the accuracy of the estimated values depends mainly on the chosen DSD type. The chart of  $\lambda_R(\text{dB/km})$  for the frequency range of 1 - 1000 GHz is shown in Fig. 1. It was generated by theoretically calculating the specific attenuation for different rain rates at the chosen frequency [24].

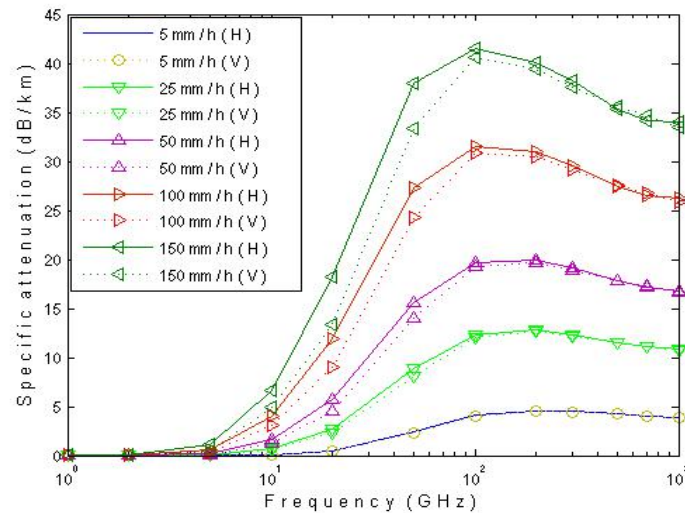


Fig. 1. ITU-R specific rain attenuation for different rain rates and frequencies

### B. Wet Antenna Attenuation

Wet antenna attenuation (WAA) depends on the factors such as the dish size, elevation angle, rain rate, wetting conditions of antenna reflector surfaces and so forth [8]. In order to evaluate the attenuation caused by water flowing on the antenna surface, the water layer thickness is predicted to be random all over the reflector. The thickness of water for a laminar flow is given by Gible's expression [7], [25]:

$$t_w = \sqrt[3]{\frac{3\mu_w r R}{2g}} \quad (2)$$

where  $t_w$  (mm),  $\mu_w$  ( $m^2/s$ ),  $r$  (m),  $R$  (mm/h), and  $g$  ( $m/s^2$ ) are the water layer thickness, viscosity of water, radius of reflective surface, rain rate and gravitational acceleration, respectively.

WAA  $A_w$  (dB) is estimated from the difference in the receive signal levels during dry and wet conditions. For instance, let  $\psi_1$  and  $\psi_2$  represent the received signal levels in dry and wet antenna (WA) conditions in dBm, respectively, therefore the attenuation is expressed as

$$A_w = \psi_1 - \psi_2 \quad (3)$$

The rainfall rate data from few selected tropical and equatorial climates [24], [26], shown in Fig. 2, were employed in (2) to study the behavior of water thickness; and the results are shown in Fig. 3 and Fig. 4. For instance, the plots of water thickness versus time percentage rainfall rate is exceeded are shown in Fig. 3, while the behavior of the water thickness with respect to rainfall rate is shown in Fig. 4. The equiprobable plots of water thickness against rainfall rate are presented in Fig. 4 for the respective exceedance probability, where it is observed that, the water thickness increases with increasing rain rate. These results further justify the common trend shown by both rainfall rate and water thickness where the two quantities increase with decreasing exceedance probability.

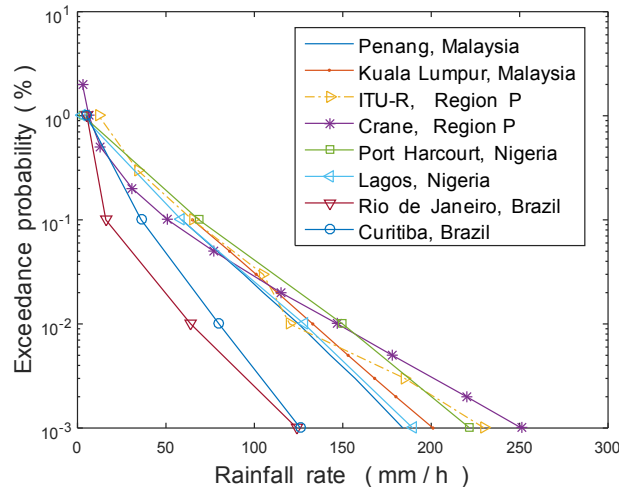


Fig. 2. Rainfall rate exceedance

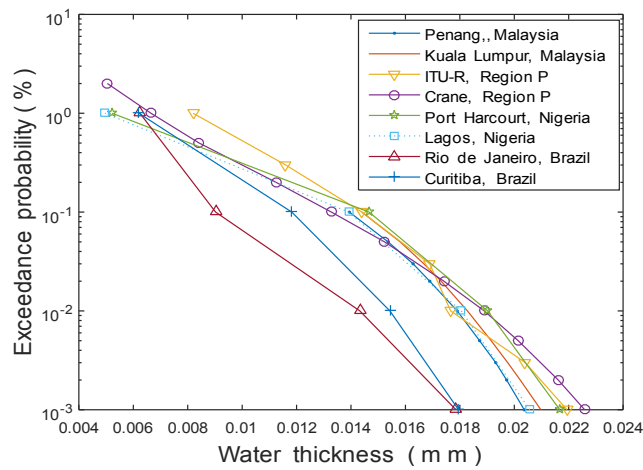


Fig. 3. The plots of water thickness for a laminar flow, dish diameter=0.6m versus time percentage rainfall rate is exceeded

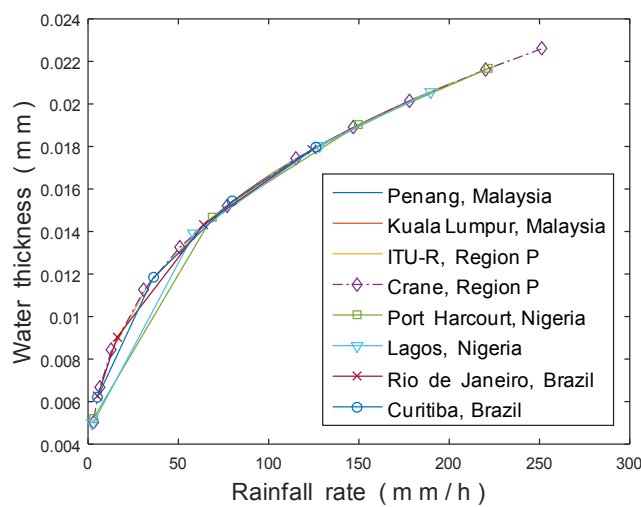


Fig. 4. Equiprobable plots of water thickness versus rain rates for a laminar flow, dish diameter=0.6m.

### III. METHODOLOGY

Detailed descriptions of the interconnections of the digital satellite receiver and the personal computer, as well as the experiments carried out are presented in the following subsections.

#### A. Descriptions of Digital Satellite Receiver

The experiment was carried out in Ilorin, a tropical climate and the state capital of Kwara State, Nigeria ( *Lat.*8.4912°N; *Long.*4.5950°E; Altitude is 317 m above sea level). The average annual temperature and rainfall are 26 °C and 1232.8 mm, respectively. The experimental set up consists of parabolic antenna, with a universal type LNB, a TBS–QBOX device (Digital satellite Receiver) and a personal computer for a user interface. The LNB was connected to a TBS–QBOX using coaxial cable; the TBS–QBOX was connected to a PC using a USB cable as shown in Fig 2. The receiving antenna was set looking towards the geostationary satellite Eutelsat 36A at 36°E longitude with satellite beacon footprint at 11.843 GHz, vertically polarized. The propagation characteristics of the measurement site are shown in Table I.

TABLE I: PROPAGATION CHARACTERISTICS OF THE MEASUREMENT SITE

Frequency of the downlink signal	11.843 GHz
Polarization	Vertical
Antenna elevation angle	42°
Latitude	8.4912 °N
Longitude	4.5950 °E
Height of antenna	3.9m
Diameter of antenna	0.6m

#### B. Rain Simulator and Water Spray Experiments

As shown in Fig. 5, the rainfall simulator consists of PVC bored pipes mounted on a wood construction, which were connected to a water source through a rubber tube. The water source was controlled so as to simulate different rain rate intensities. A tipping bucket rain gauge fitted with a wireless programmable data logger was used for the rain rate data collection. The simulated rain experiments were carried out on the receiving antenna of an offset antenna reflector surface. As a reference, the test was first carried out on clear-sky weather conditions in order to calibrate the receive signal level (RSL) by the receiver.

The WA experiments conducted comprised four types. Water droplets characterized with very low rainfall intensities (typically, less than 8 mm/h) were sprayed in the first test to ensure uniform distribution on the antenna reflecting surface. In the second test the flow rate of the simulated rain was adjusted to 10 - 45 mm/h down-flow of water droplets a few millimeters wide. The antenna was sprayed with higher intensities of water in the third test, ranging from 50 mm/h to 110 mm/h. Finally in the fourth test, the heaviest intensities of water (greater than 120 mm/h) was simulated by splashing and allowed to flow down across the antenna surface. The spraying processes were repeated thrice for

each of the four tests conducted after the surface has dried out. In each of the four scenarios, it was observed that the antenna losses increase with increasing rain rate.

The WAA  $A_{W,0.01}$  for the four spraying tests were measured and the results were used to estimate the attenuation  $A_{W,p}$  (dB) exceeded for other time percentages,  $p$  by using the extrapolation formula of the ITU-R P. 618-17 [27],

$$A_{W,p} = A_{W,0.01} \left( \frac{p}{0.01} \right)^{-(0.655 + 0.033 \ln(p) - 0.045 \ln(A_{W,0.01}) - \beta(1-p) \sin \theta)} \quad (4)$$

$$\text{If } \begin{cases} p \geq 1\% \text{ and } |\varphi| \geq 36^\circ; \beta = 0 \\ p < 1\% \text{ and } |\varphi| < 36 \text{ and } \theta \geq 25^\circ \beta = -0.005(|\varphi| - 36) \\ \text{otherwise; } \beta = -0.005(|\varphi| - 36) + 1.8 - 4.25 \sin \theta \end{cases} \quad (5)$$

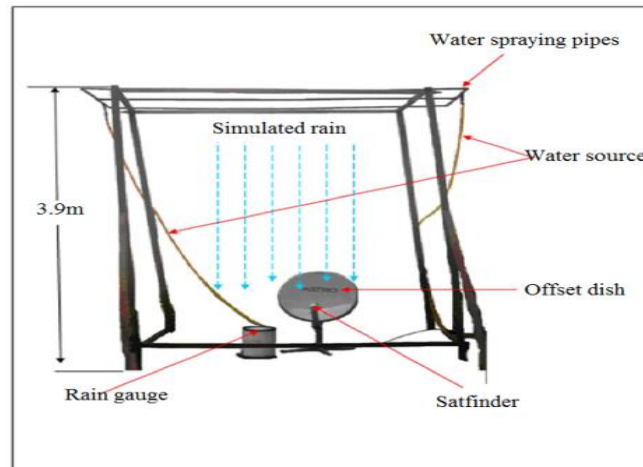


Fig. 5. Rain simulator set-up

#### IV. RESULTS AND DISCUSSION

##### A. Analysis of the results of raw measurements

Water sprayer tests were conducted in order to measure the total rain attenuation, comprising the effects of rain on propagation path and on WA. The cumulative distributions of total, excess and WA attenuations are shown in Fig. 6. The measured total rain attenuation recorded were 5.36, 12.0, and 19.57 dB for 0.1%, 0.01%, and 0.001% of the occurrence, respectively. When the results of the splashing test were carefully analyzed, it was inferred that the values responsible for WAA were 1.13, 2.98 and 6.3 dB at the afore-mentioned corresponding time percentages. These values are too significant and must not be allowed to misrepresent the actual values of measured rain attenuation for assurance and guarantee of proper link budgeting, which consequently translates to acceptable quality of service.

The WA attenuation statistics for different spray tests are shown in Fig. 7, where the losses range from 0.22 dB (rivulet tests) to 2.98 dB (heavy spray tests) at water film thickness of 0.15mm and 11.843 GHz. This evidently shows that the antenna losses vary with the spraying intensities. The

maximum WA loss recorded (with the splashing test) was approximately 2.98 dB at 0.01%. Note that the value is comparable with the results of similar tests carried out at USM, Malaysia (Engineering Campus), UTM, Malaysia (Johor Campus), near Singapore and in some other published works. For instance as shown in Fig. 8, the maximum corresponding WA losses recorded at USM [28] and UTM [16] on the 12.4 and 14.6 GHz links were respectively 3.08 and 2.6 dB.

The losses recorded at British Columbia University, UBC, Vancouver, Canada [1], [12] and UTM [11] on the 20.2 and 18.585 GHz links, respectively were 4.5 and 3.4 dB. The slight differences observed between the experimental results in this study and those reported in the reviewed works can be explained as follows: the antenna elevation angle used in Malaysia was  $51^\circ$ , while  $42^\circ$  was used in our experiment. Thus, the losses should be expectedly higher for the latter scenarios compared to the former, depending on the operating frequencies and polarizations.

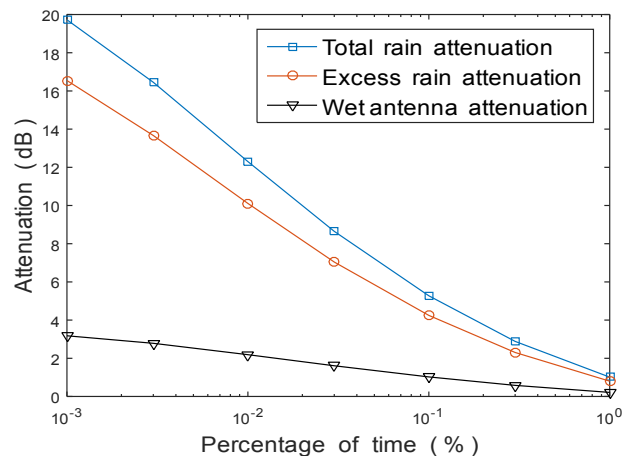


Fig. 6. Cumulative distributions of total, excess and WAAs

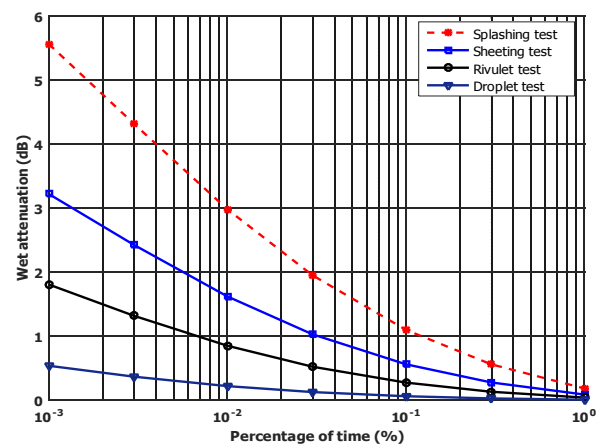


Fig. 7. Cumulative distributions of WAA for different spray tests

### B. Comparison of frequency-scaled results with other tropical locations

The experimental results reported in this work were measured at a lower frequency (11.843 GHz), compared to other sites reported in a few of the reviewed works. For instance, refer to the links' frequencies at UBC, Canada (20.2 GHz) and UTM, Malaysia (18.585 GHz). Due to this reason, the

frequency scaling technique [29] has been used to scale up the measured attenuation being currently reported in this work (11.843 GHz) to the corresponding values at the desired frequencies. This will be a justification for comparing our results with those reported in UTM, Malaysia and UBC, Canada. Most of the widely used models for tropical climates are based on the power over the ratio of frequencies and statistical attenuation ratio (RAS). Therefore, the simple power-law model was used [30].

$$RAS_n = \frac{A(f_U)}{A(f_L)} = \left(\frac{f_U}{f_L}\right)^n \quad (6)$$

where  $A(f_L)$  and  $A(f_U)$  are the equiprobable values of the WAA at the lower frequency  $f_L$  and upper frequency  $f_U$ , respectively.

The proposed values for power  $n$  across 12 - 30 GHz frequency range are presented in Table II [24]. The simple power-law model of (6) was used to scale up the measured attenuation from 11.843 GHz to (i) 18.585 and (ii) 20.2 GHz, for predicting the corresponding values at these frequencies. Both the measured and frequency-scaled WAAs were compared with those reported from Canada and Malaysia as shown in Fig. 8 and Fig. 9. The results of the work presented are in the same trend with the few selected tropical and equatorial climates.

TABLE II. VALUES OF POWER  $n$  FROM VARIOUS RESEARCHERS [24]

Model	Frequency pair $f_U/f_L$	$n$
Drufuca (1974)	19/11	1.72
Ajayi and Owolabi (1982)	20/12; 30/12	2.0
Dintelmann	30/20	1.8
OLYMPUS	20/12; 30/20; 30/12	1.9

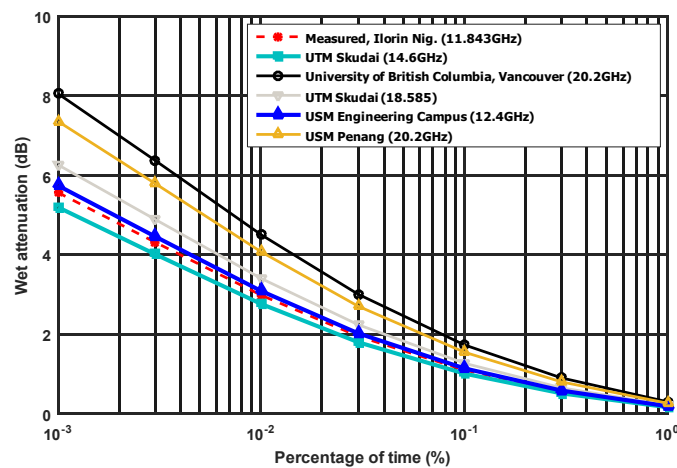


Fig. 8. Comparison of measured wet attenuation with those reported from Canada and Malaysia

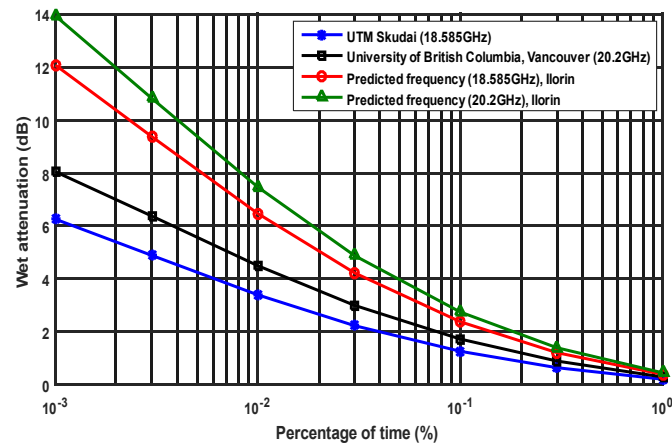


Fig.9. Comparison of WAA (frequency-scaled at 18.585 and 20.2 GHz) with those reported from Canada and Malaysia. Equation (2) was further investigated by finding its gradient with respect to (wrt) rainfall rate, thereby yielding the following expression

$$\frac{d t_w}{d R} = \frac{1}{3} \sqrt[3]{\frac{3 \mu_w r}{2 g}} r^{1/3} R^{-2/3} \quad (7)$$

Let  $\xi(R) = \frac{d t_w}{d R}$ , then (7) reduces to

$$\xi(R) = 0.4807 \left( \frac{\mu_w r}{2 g} \right)^{1/3} R^{-2/3} \quad (8)$$

Equation (8) was used to study the effects of the water thickness gradient  $\xi(R)$  on the radio-wave propagation as shown in Fig. 10. The results of curve-fitting analysis on this figure show that  $\xi(R)$  can numerically be defined as a simple power-law function, given as

$$\xi(R) = 0.0123 R^{-0.667} \quad (9)$$

Compared with the results shown in Fig. 3, the water thickness gradient decreases with increasing rain rate, (see (9)). The parameter  $\xi(R)$  has the dimension of time, and it may be interpreted as the total time duration during which a particular rainfall rate will cause a given amount of water thickness to be accumulated on the antenna surface. The relation between the rainfall intensity and the thickness of the water layer formed on link antennas is, of course, dependent on the type of antenna (e.g., shape, cover material), the wind direction, surrounding obstacles, etc. The range of thickness of water layer is 0.0052 – 0.0217 mm corresponding to rainfall rate of about 3 – 221 mm/h. It should however be noted that, more intense rain events, with more water falling on the antenna do not necessarily imply more water being retained on the antenna surface, and hence a thicker water layer [24]. The thickness of water layer is largely dependent on the buildup and runoff of water on the surface; that is the higher the rain rate the faster the process of buildup and runoff.

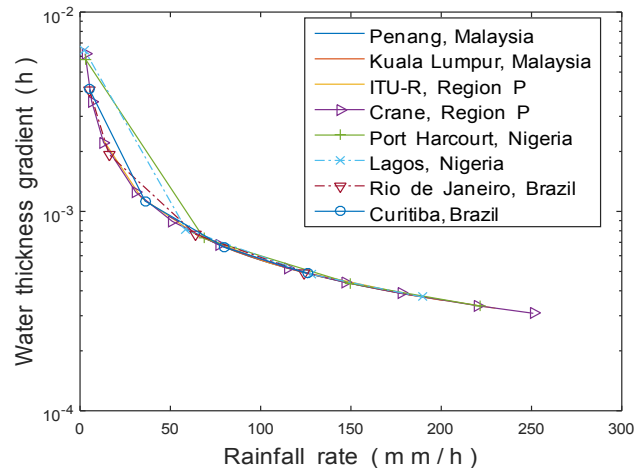


Fig. 10. Plots of water thickness gradient for a laminar flow, dish diameter = 0.6 m.

The behaviour of  $\xi(R)$  for various dish sizes is illustrated in Fig. 11, and it is clearly seen that its value increases with increasing dish size for the same amount of rain rate. The characteristics of the sites used for illustrations in Figs. 2, 3, 4 and 10 are shown in Table III.

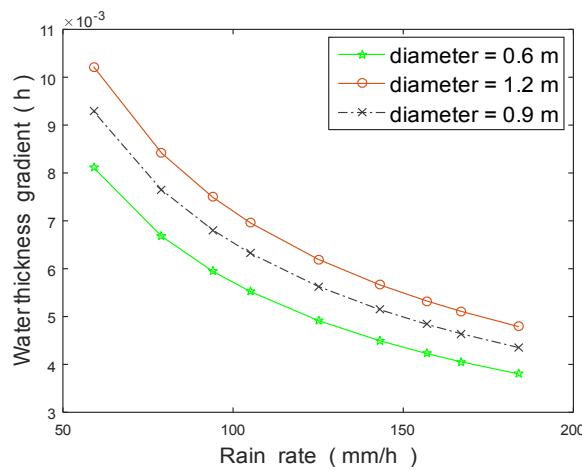


Fig. 11. The behaviour of  $\xi(R)$  for various dish sizes.

TABLE III. CHARACTERISTICS OF SITES USED FOR ILLUSTRATIONS

S/N	Sites	Latitude	Longitude	Altitude (m)	$R_{0.01}$ (mm/h)
1	Penang, Malaysia	5.4141 °N	100.3288 °E	57.0000	135.0000
2	Kuala Lumpur, Malaysia	3.1390 °N	101.6869 °E	21.9500	133.0000
3	Lagos, Nigeria	6.6018 °N	3.3515 °E	38.0000	128.1400
4	Port Harcourt, Nigeria	4.8156 °N	7.0498 °E	18.0000	149.8800
5	Rio de Janeiro, Brazil	22.9068 °S	43.1729 °W	10.0000	128.0000
6	Curitiba, Brazil	25.4372 °S	49.2700 °W	935.0000	126.0000
7	ITU-R, Region P	-	-	-	120.0000
8	Crane, Region P	-	-	-	147.0000

## V. CONCLUSION

The results of the rain simulation experiments conducted on a receiving parabolic antenna show that the wetting effect on antenna could produce significant attenuation in addition to path attenuation, thereby contaminating the actual path attenuation. The measured wet-antenna attenuation is as high as 2.98 dB at 11.843 GHz, for heavy rain rates (160 mm/h). WA effects could be more severe at higher frequencies and lower elevations, depending on the rainfall rates, drop size distribution (DSD), polarization and other propagation characteristics. More so, antenna surface may be deteriorated during long term outdoor usage, thereby causing thicker water layer on its surface. This may increase the film attenuation even with the same rainfall intensity. The value of instantaneous attenuation is determined by water-layer thickness on the antenna surface at any instant of time. Water film attenuation increases with thicker water film and higher radio frequency. The parameter  $\xi(R)$  may be interpreted as the total duration of time during which a given amount of water thickness, corresponding to a particular rainfall rate, will be accumulated on the antenna surface. The behavior of  $\xi(R)$  for various dish sizes was also investigated; and it was found that its value increases with increasing dish size for the same amount of rain rate. The study is useful to the radio designer engaged in accurate link budget estimations for reliable quality of service (QoS).

## ACKNOWLEDGMENT

This research is supported by the Antenna and Radio Propagation Group, (A&RPG), Department of Electrical and Electronics Engineering, University of Ilorin, Ilorin, Nigeria.

## REFERENCES

- [1] R. K. Crane, "Rain Attenuation Models: Attenuation by Clouds and Rain," In Propagation Handbook for Wireless Communication System, CRC Press, United States of America, pp.225-280, 2003.
- [2] J. Pastorek, M. Fencil, J. Rieckermann and V. Bares, "Precipitation Estimates from Microwave Links for Urban Hydrology: Improving the Accuracy Using Wet-Antenna Calibration," *2021 8th International IEEE Conference on Microwaves, Communications, Antennas, Biomedical Engineering and Electronic Systems – CELLular ENvironment MONitoring (CELLENMON) Special Session*, pp.1-9, 2021.
- [3] B. Blevis, "Losses due to rain on radomes and antenna reflecting surfaces". *Antennas and Propagation, IEEE Transactions on*, vol. 13, pp. 175-176, 1988.
- [4] B. B. Jimoh, A. Y. Abdulrahman, Falade A. J., O. Oniyide, O. S. Zakariyya , T. A. Rahman, "Evaluation of Frequency Scaling Prediction Techniques using Experimental Data," *J. of Telecommunications & Radio Engineering*, vol. 76, no. 5, pp. 433 – 442, 2017.
- [5] A. Ajiboye, A. Y. Abdulrahman, A. J. Falade, A. T. Ajiboye, O. S. Zakariyya and T. A. Rahman, "Effects of ionospheric scintillation on communication systems: GPS and satellite," *J. of Telecommunications & Radio Engineering*, vol. 76, no. 20, pp. 1849-1859, 2017.
- [6] A. Y. Abdulrahman, A. Falade, B. J. Olufeagba and O. O. Mohammed, "Statistical evaluation of measured rain attenuation in tropical climate and comparison with prediction models," *Journal of Microwave, Optoelectronics and Electromagnetic Applications*, vol. 15, no. 2, pp. 123 – 134, 2016.
- [7] S. K. A. Rahim, A. Y. Abdulrahman, T. A. Rahman, M. R. Islam, "Measurement of Wet Antenna Losses on 26 GHz Terrestrial Microwave Link in Malaysia," *Wireless Personal Commun*, vol. 64, pp. 225-23, 2010.
- [8] C. Moroder, U. Siart, C. Chwala, and H. Kunstmann, "Fundamental Study of Wet Antenna Attenuation," 1-4, *15th International Conference on Environmental Science and Technology, Rhodes, Greece*, pp. 1 – 4, 2017.
- [9] J. Polz, C. Chwala, M. Graf, and H. Kunstmann, "Rain event detection in commercial microwave link attenuation data using convolutional neural networks," *Atmos. Meas. Tech.*, vol. 13, pp. 3835–3853, 2020.
- [10] J. Y. C. Cheah, "Wet antenna effect on VSAT rain margin," *IEEE Transactions on Communication*, vol. 8, no. 41, pp. 1238-1244, 1993.
- [11] M. M. Z. Kharadly, R. Ross, "Effect of wet antenna attenuation on propagation data statistics," *IEEE Transactions on Antennas and Propagation*, vol. 49, no.8, pp. 1183-119, 2001.
- [12] R. K. Crane, X. Wang, D. B. Westenhaver, W. J. Vogel, "Acts propagation experiment: experiment design, calibration, and data preparation and archival", *Proceedings of the IEEE*, vol. 8, no. 6, pp. 863–877, 1997.

- [13] R. J. Acosta, R. R. Reinhart, D. Kifer, C. Emrich, Goldshan, “Wet antenna studies on LeRC, *Proceedings of the 21<sup>st</sup> NASA Propagation Experimenters (NAPEX XXI) Conf.*”, California institute of Technology, El-Segundo, California, USA., June 1997.
- [14] A. Overeem, H. Leijnse and R. Uijlenhoet, “ Measuring urban rainfall using microwave links from commercial communication networks,” *Water Resour. Res.*, vol. 47, no. 12, pp. 1 - 16, 2011.
- [15] M. Schleiss, J. Rieckermann and A. Berne, “Quantification and modeling of wet-antenna attenuation for commercial microwave links,” *IEEE Geosci. Remote Sens. Lett.*, vol. 10, no. 5, pp. 1195 – 1199, 2013.
- [16] M. R. Islam, A.R. Tharek, J. Din and J. Chebil, “Measurement of wet antenna effects on microwave propagation - an analytical approach” Microwave Conference, Asia-Pacific, pp. 1547-1551, 2000.
- [17] J. Ostrometzky, R. Raich, L. Bao, J. Hansryd and H. Messer, “The wet antenna effect- a factor to be considered in the future communication networks,” *IEEE, Transactions on antenna and propagation*, vol. 66, no. 8, pp. 315 – 322, 2018.
- [18] M. F. Rios Gaona, A. Overeem, T. H. Raupach, H. Leijnse, and R. Uijlenhoet, “Rainfall retrieval with commercial microwave links in São Paulo, Brazil,” *Atmos. Meas. Tech.*, vol. 11, no. 7, pp. 4465–4476, 2018.
- [19] M. Fencel, P. Valtr, M. Kvicera and V. Bares, ”Quantifying wet antenna attenuation in 38 GHz commercial microwave links of cellular backhul,” *IEEE, Geoscience and Remote sensing Letter*, vol. 16, no. 4, pp. 514 – 518, 2019.
- [20] N. David, O. Harel, P. Alpert and H. Messer, “Study of attenuation due to wet antenna in microwave radio communication,” *IEEE International Conference on Acoustics, Speech and Signal Processing (ICASSP)*, pp. 4418-4422, 2016.
- [21] D. Cherkassky, J. Ostrometzky and H. Messer, “Precipitation classification using measurements from commercial microwave links,” *IEEE Transactions on Geoscience and Remote Sensing*, vol. 52, no. 5, pp. 2350 – 2356, 2014.
- [22] C. Moroder, U. Siart, C. Chwala, and H. Kunstmann, “Modeling of wet antenna attenuation for precipitation estimation from microwave links,” *IEEE, Geoscience and Remote sensing Letter*, vol. 17, no. 3, pp. 386 – 390, 2020.
- [23] ITU-R, Geneva, Switzerland, “Specific attenuation model for rain for use in prediction methods,” *Recommendation ITU-R P.838-3*, 2005.
- [24] A. Y. Abdulrahman, “Development of terrestrial rain attenuation transformation model for slant-path attenuation predictions in tropical region,” A thesis submitted in fulfilment of the requirements for the award of the degree of Doctor of Philosophy (Electrical Engineering) at Faculty of Electrical Engineering, Universiti Teknologi Malaysia, UTM, Malaysia, 2012.
- [25] I. Andersen, “Measurement of 20 GHz transmission through a radome in rain,” *IEEE Transactions on Antenna and Propagation*, vol. 23, pp. 619-622, 1975.
- [26] M. S. Pontes, L. A. Da Silva Mello, R. S. L. Souza and E. C. B. Miranda, “Review of Rain Attenuation Studies in Tropical and Equatorial Regions in Brazil,” *Proceeding of the 5<sup>th</sup> International Conference on Information, Communications and Signal Processing (ICICSP '05) IEEE Xplore*. Bangkok, 2005.
- [27] ITU-R Recommendation. Propagation Data and Prediction Methods required for the Design of Earth-Space Telecommunication Systems. International Telecommunication Union Geneva (Switzerland). pp. 618-10, 2017.
- [28] J. S. Mandeep, “Analysis effect of water on a Ka-band antenna”, *Progress in Electromagnetic Research Letters*, vol. 9, pp. 49-57, 2009.
- [29] M. R. Islam, “Frequency Scaling Techniques for Rain Attenuation Prediction on Terrestrial Microwave Links in Tropical Climate” *2nd International Conference on Electrical and Computer Engineering*, Bangladesh, 2002.
- [30] WCRL. Final Reports on Rain Attenuation Studies for Communication Systems Operating in Tropical Regions, Wireless Communication Research Laboratory. Universiti Teknologi Malaysia, (UTM), Malaysia, October 31, 2000.